Istraživanja i projektovanja za privredu
ISSN 1451-4117
DOI:10.5937/jaes0-41037
www.engineeringscience.rs

iipp publishing

Journal of Applied Engineering Science
Vol. 21, No. 2, 2023
Original Scientific Paper
Paper number: 21(2023)2, 1099, 577-586

ASSESSMENT OF FRICTION STIR WELDING JOINTS OF AA2017-T4 ALUMINUM BY DISC PRESSURE MECHANICAL TESTS

Abderrahmane Djili[1], Boudjema Bezzazi[1], Mohamed Habouss[2], Nadjet Zioui[3]*

[1] Unité de Recherche-Matériaux Procédés et Environnement - UR MPE Université M'hamed Bougara, Boumerdès, Algeria
[2] LSPM-CNRS UPR3407, Université Sorbonne Paris Nord, 93430 Villetaneuse, France
[3] Department of Mechanical Engineering, Université du Québec à Trois-Rivières, Canada
** nadjet.zioui@uqtr.ca*

Precipitation hardening aluminium alloy sheets AA2017-T4 are welded by FSW on a conventional FSW tool. A macrograph of the cross section of the butt-welded joint shows the classical zones for such welding, namely the nugget zone, the thermo-mechanically affected zone and the heat affected zone. Scanning Electron Microscopy displays a grain refining and a re-formation of the precipitates in the nugget zone. Micro-hardness measurements on the cross-section perpendicular to the welding direction give the standard W-profile of the hardness for such welding, with as expected, the relatively highest value at the joint center (nugget zone). To assess the mechanical performance of the FSW welded joint, the Disk Pressure Test (DPT) is used. It shows a failure pressure for the welded specimen that is 17% lower than the base material. The fracture surface micrographs clearly show a thickness reduction at break that is ~36% higher for the base material than the welding joint and a ductile fracture mode for both specimens.

Keywords: FSW, Aluminium alloy, tensile mechanical test, Disk Pressure Test (DPT)

1 INTRODUCTION

Since its advent in the 1990's at the welding institute (England), [1], the friction stir welding (FSW) has proven its efficiency in welding similar or dissimilar materials, which are known to be either difficult or even impossible to weld by other conventional fusion welding techniques. Examples of such materials are metallic alloys like aluminum, titanium [2] and copper or dissimilar materials like aluminum/magnesium, aluminum/copper, and aluminum/stainless steel [3] or even polymers, [4,5].

FSW is a solid-phase welding process that operates by plunging the pin of a specially designed rotating tool, made of harder material, between the materials to be welded, and fractioning these materials with the rotating tool, so as to generate enough heat for softening the materials and mix them to create the welding joint. This latter can be of butt, lap or spot type. FSW stands as a versatile and eco-friendly technique as it enables to assembly different types of materials, without requiring neither depositing extra material nor other consumable for welding materials [3].

The quality of the FSW joint in term of mechanical performance is assessed by comparison to the base materials (BM). It is a consequence of the joint microstructure state that is dependent of two complex phenomena, induced by the FSW process, which are the mechanical locking and the dynamic recrystallization of BM. These latter are due to the severe deformation and the generated frictional heat, which occur at the welding zones in a way monitored by the FSW process variables that are the machining parameters [6], the welding tool characteristics [7], clamping system and the BM properties. The process parameters are the tool rotational speed (ω), the tool advance speed (V) (for the butt or lap joint welding), the tool offset, the tool shoulder tilt angle (α), the time of tool dwelling, and the tool plunging depth (dp) [8]. The welding tool characteristics comprise the shoulder diameter (ϕs), the shoulder topology (convex or concave), the pin diameter (ϕd), the pin topology (shape, threaded or not), and the pin length. Finally, the base material properties are the ones governing its mechanical and thermal behavior (hardness, stiffness, conductivities, etc.).

Optimizing the mechanical performance of the FSW joint with respect to some of the processing parameters (considering the whole parameters in once seems difficult) has been the subject of numerous works in the last three decades. In their large majority, the mechanical performance is assessed by measuring the ultimate tensile strength (UTS) and the ultimate elongation (UE) based on a uniaxial tensile mechanical test. Some recent examples of such works, related, to the assessment of the quasi-static mechanical strength of the FS Welding of aluminum alloys in butt joint, are given in [9-10].

In [11] the authors investigate the effects of ultrasonic vibration on the microstructures and mechanical properties of dissimilar FSWed joints. It has been shown that the application of ultrasonic vibration reduces the thickness of intermetallic compounds and improve the joint tensile strength. Also, the ball-burnishing process improves the mechanical properties of friction stir welded joint by increasing the material hardness and decreasing the compressive residual stresses [12].

In [9-13], the authors investigate the effect of the tool traverse (V) and spindle speeds (ω) on the microstructural evolution and mechanical properties (UTS, UE) of FSWed aluminum alloys with special emphasis on the hardening capacity and the effect of post-welding aging treatment in references [14] and [15], respectively. In [16], the influence

of the tool dwelling time, besides ω and V, was examined, on UTS, UE and the axial force as well. In [17], the authors studied the influence of the polygonal pin profiles on the material flow, the microstructure, and the mechanical properties (UTS, UE) of (6082) aluminum alloy FS Welds. In [18], the authors investigate the role of pin eccentricity in friction stir welding and conclude that pin eccentricity further improves grain refinement in the agitation zone and improves the toughness of the FSWed joint. In [19] the author shows that the material properties of the tool have a direct effect on the mechanical properties of the FSWed joint. The clamping system also influences the FSWed joint properties; in [20] the author demonstrates the effect of the clamping distance on the grain structure evolution, precipitate distribution, and tensile properties of the FSWed joint. In [21] the authors confirm the effect of backing and cover materials of clamping system on the FSWed joint strength.

In [22], the Limiting Dome Height (LDH) biaxial test was used to investigate the forming performance, the formability of a welded joint is compared to base materials. In [23], authors propose an optimization study of the FSW process parameters which gives the maximum responses of the dome height.

In [10], the mechanical performance of the FSWed AA2024-T4 aluminum sheets, at 400°C temperature, was assessed by uniaxial and biaxial free bulging tests. Hence, among the quoted references, only three, [10-22-23], used biaxial test to investigate the quasi-static mechanical strength of FSWed joint. In fact, uniaxial tensile mechanical test is extensively used to assess the mechanical performance of the FSW joint, and there is only very few works employing biaxial mechanical tests, among which those cited here [10-22-23], despite the obvious relevance of biaxial assessment of FSWed aluminum sheets dedicated for example, to potential storage and/or transport applications of fluid or gas.

Thus, it is proposed in the present work, to use a specific bi-axial mechanical test, namely the Disc Pressure Test (DPT), in addition to the tensile test, to assess the mechanical performance of FSWed joints of precipitation hardening aluminum alloy sheets of 2017-T4.

The DPT [24] consists in loading an embedded thin disk with an increasing gas (helium or argon) pressure at constant rate until the disk bursts or cracks. It is used among all for the qualification of metallic alloys dedicated to hydrogen storage application following the ISO standard 11114-4:2008 [25].

To conduct this study, aluminum alloy sheets AA2017-T4 are first FS welded on conventional FSW tool, by using a cylindrical tool made of Z200C12 hot-work steel that was specially designed for this purpose. The welded material belongs to the class of precipitation hardening aluminum alloys that possess good specific (related to weight) mechanical properties, which justify their intensive utilization in various applications like aeronautical, nuclear and transport, but are known as to weld by conventional fusion welding technique.

The process parameters are selected by examining the literature on this subject, to ensure the best quality joints. Hence, the adopted parameters agree well with the findings of references [26] and [27], based on multicriteria optimization and empirical relationship. Besides the tensile and DPT mechanical testing to assess the mechanical performance of the welds, additional local analyses are performed, namely the Scanning Electron Microscopy analysis and hardness measurement, for characterizing the evolution of the microstructure at different areas of the welding joint, viz. the thermo-mechanically affected zone (TMAZ), the nugget zone (NZ), and the heat affected zone (HAZ).

The paper is organized as follows: In section 2 the used material and the experimental procedures for welding, mechanical testing and micro-graphical and local characterizations are presented. Section 3 is dedicated to the presentation and comparison of the obtained results for the base metal and welded joints, regarding the mechanical properties, the microscopic imaging, the hardness measurement, and the fracture facies. Finally, the main findings and conclusions of the study are presented in section 4.

2 EXPERIMENTAL

2.1 Material and welding

Two millimeters thick sheets of precipitation hardening aluminum alloy AA2017-T4 purchased in the market are used in this study. The chemical composition and the mechanical properties of the material, provided by the supplier, are summarized in Tables 1 and Table 2.

Table 1. Chemical composition (% mass) of AA2017-T4 aluminum alloy

Element	Si	Fe	Cu	Mn	Mg	Zn	Ti	Cr	Al
Percent	0.71	0.3	4.2	0.7	0.74	0.22	0.05	0.05	Bal.

Table 2. Mechanical properties of the used aluminum AA2017-T4 alloy

	Tensile strength (MPa)	Yield strength (MPa)	Elongation (%)
AA2017-T4	437	305	18

Samples of 70x150mm size are cut with a lever shear before being friction stir welded (butt joints) in the rolling direction. The welding was carried out with a conventional FSW tool (See Fig. 1a) by using a specially designed refractory tool that was fabricated on purpose from a hot-work steel (X210Cr12) material. For welding, the rotating tool pin is first plunged into the butt joint of the welded sheets. After a short dwelling time, the tool is moved forward along the butt joint line. Process parameters such as tool geometry, traverse and rotational speeds directly influence the quality of the welding joints. In this study, these parameters were selected to obtain satisfactory joints, free from

defects that are due to improper flow and insufficient consolidation of metal in the friction stirring zone (NZ). The dimensional and geometrical details of the tool are given in Fig. 1c. The adopted welding speed (V) and the tool rotational speed (ω) are fixed at 80 mm/min and 1140 rpm, which agree well with references [26] and [27], where multicriteria decision making techniques and Response Surface Methodology have been used, respectively, to find the optimal values of process parameters (ω, V). Moreover, the tool tilt angle is fixed at 1.5° for all the welds in this study. The welding was performed at room temperature. The sample advancing and retiring sides are presented in Fig. 1b. A post-welding inspection of the welds shows no apparent macro-defects at the surface.

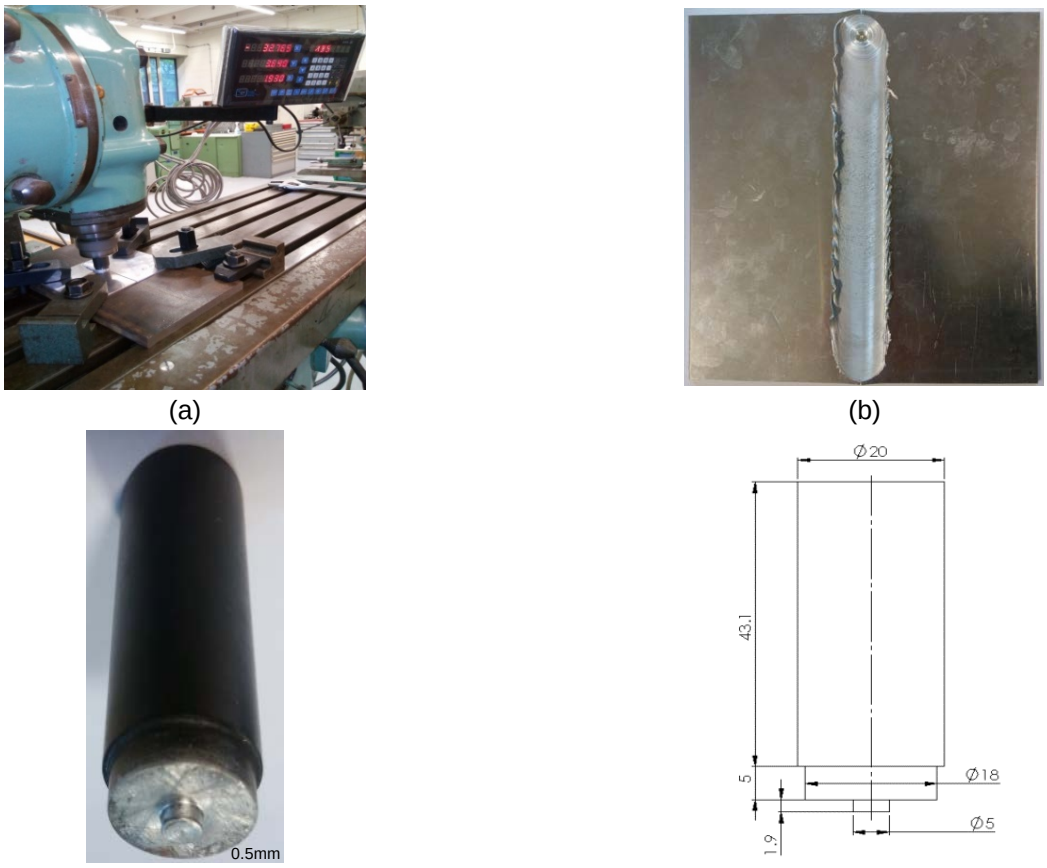

(a) (b) (c) (d)

Fig. 1. Friction stirs welding process: a) Milling machine with the tool mounted and the alloy plates clamped in place, b) Appearance of a fresh friction stir weld, c) The welding tool, d) Tool dimensions

2.2 Macro- and micro - scopic characterization

The macrograph allowed to have a global view of the joints with the different resulting zones as well as their limits, while the micrographs show the grain sizes and the precipitates distribution, for this samples were cut perpendicular to the welded joints (See Fig. 2), before being mechanically polished, with abrasive papers of different grades, according to metallographic standards, and chemically etched with Keller's reagent (2.5% HNO3, 1.5% HCl, 1% HF and 95% H2O). A macroscope was used for the macrograph and a scanning electron microscope (SEM) was used to probe the sample surface of nugget zone (NZ) and base metal (BM). Special attention was given to the fracture surface after the disc pressure test of welded and BM sample to identify the nature (brittle or ductile) of the failure.

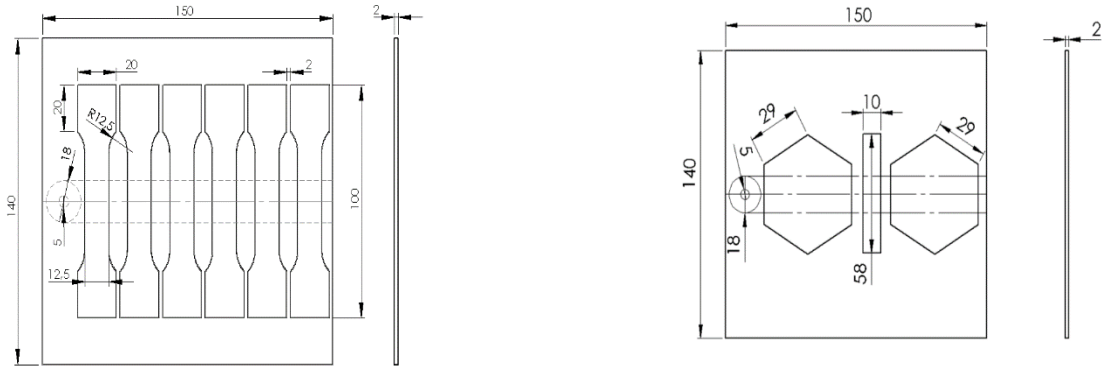

(a) (b)

Fig. 2. Scheme for extracting test coupons from the friction-stir-welded aluminum alloy plates a) Tensile test coupon, b) Disc pressure test coupon

2.3 Micro - hardness test

A hardness profile through the FSWed joint gives the possibility of connecting the micrographs of different zones and their mechanical characteristics. The Vickers microhardness was measured in the test coupon cross section cut perpendicular to the weld. An automatic Micro-HMV2 hardness tester was used. The indentation load was 0.5 kg, and the loading time was 15 s. The measurements were performed at a depth of 1 mm with a 1 mm gap between measurements.

2.4 Tensile test

In order to compare the tensile characteristics (Tensile strength, Yield strength and elongation) of the FSW welds and the base metal, several tensile tests were carried out. Tensile standard specimens were cut perpendicularly to the welding joint, according to ASTM E8 standard [28] as illustrated in Fig. 2. The tensile mechanical test has been performed with an MTS-20M tensile machine - 100 kN loading cell under displacement loading control. A traverse speed of 0.1 mm/s was applied during all the tests carried out, until failure. The tests were conducted at room temperature (~20°C).

2.5 Disc pressure test

The performance and failure mechanism of FSW welds under biaxial loading are the objectives of performing the disc pressure test. The disc pressure test (DPT) specimens were prepared from the welded sheet and the as-received base material (BM). The specimens of the DPT are polygonal and mechanically polished on both sides until they are 1.2 mm thick (0.4 mm removed on each side). This thinning operation aims to eliminate the thickness variation generated by FSW welding and hence, avoid the resulting phenomenon of stress concentration. The shape and size of the specimens are shown in Fig. 2.

Prior to the pressure loading, the polygonal specimen is positioned in the so-called test cell, fixed between two cylindrical steel flanges (Fig. 3). It is worth noting that the inner radius of the upper cylindrical flange has been fixed to sufficiently higher value, equal to 4.5 mm, in order to reduce the stress and strain concentration and hence, the risk of rapid failure at the contact zone between sample and ring edge. In fact, premature failure may render the test not reliable and impedes the bi-axial nature of the deformation. By avoiding such edge effects, it can be ensured that the most severe mechanical stresses are located inside the specimen (at the pole/apex for homogeneous material).

The disc pressure tests were carried out using a device that allows the application of a variable rate of pressure loading, from 10^{-3} to 10^{2} bar/s by using an inert gas. In the present experimental tests, a pressure loading rate of 25 bar/s was adopted. The pressure versus time curves is the output of the performed tests. The fractured surfaces of the tested specimens are examined using a CAMBRIDGE-360 SEM.

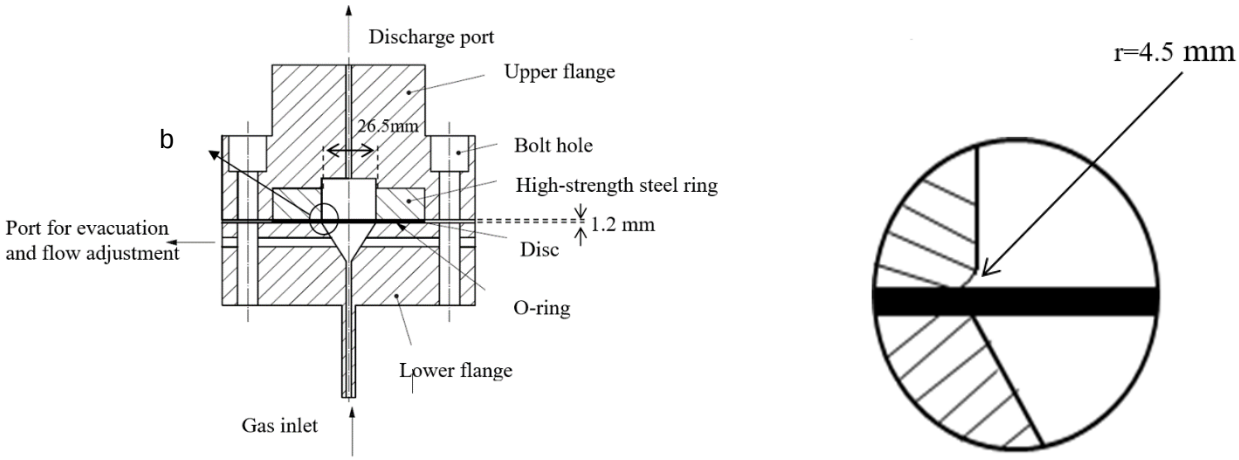

Fig. 3. Disc pressure test, a) Cross section of the test cell [25], b) Enlarged view of the beveled edge created to avoid premature failure

3 RESULTS AND DISCUSSION

A primary checking of the quality of the performed FSWed joints is based on the visual testing; Welds appeared displayed on Fig. 1.b, to be free of visible defects on the surface. The macrograph of a cross section of a friction stir weld joining AA2017-T4 aluminum alloy sheets is shown in Fig. 4. The classical zones for such joint are visible, namely the base material (a), the nugget zone (d), the thermo-mechanically affected zone (TMAZ) (b) and the heat affected zone (HAZ) (c). The larger thickness of HAZ and TMAZ in the advance side (AS) compared to the retrain side (RS) is clearly seen. It should also be noted that the joints are free from deep welding defects. The joint average thickness (1.94 mm) is here lower than that of the base metal, which is commonly observed in FSW unlike in fusion-based welding conventional techniques.

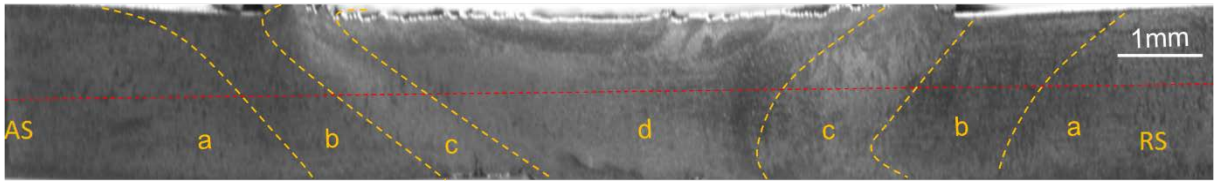

Fig. 4. Cross section of a friction stir weld in AA2017-T4 aluminum alloy. (a) Base material, (b) Thermo-mechanically affected zone, (c) Heat-affected zone, (d) Nugget zone

3.1 Micrography

In Fig. 5, the micrographs of the nugget zone in the FSW joint, and the base metal BM are displayed. It points out a finer grain size in the nugget area Fig. 5a, compared to the coarse grain size of the base metal (BM) Fig. 5b. This was expected given the severe deformation undergone by the grain inside the welding zone and the inherent dynamic recrystallization promoted by the heat, generated by the friction between the pin and mainly between the shoulder and the material. It can also be noticed that the precipitates from the base material have re-precipitated with a new distribution during FSW welding as pointed out in [29, 30, and 31].

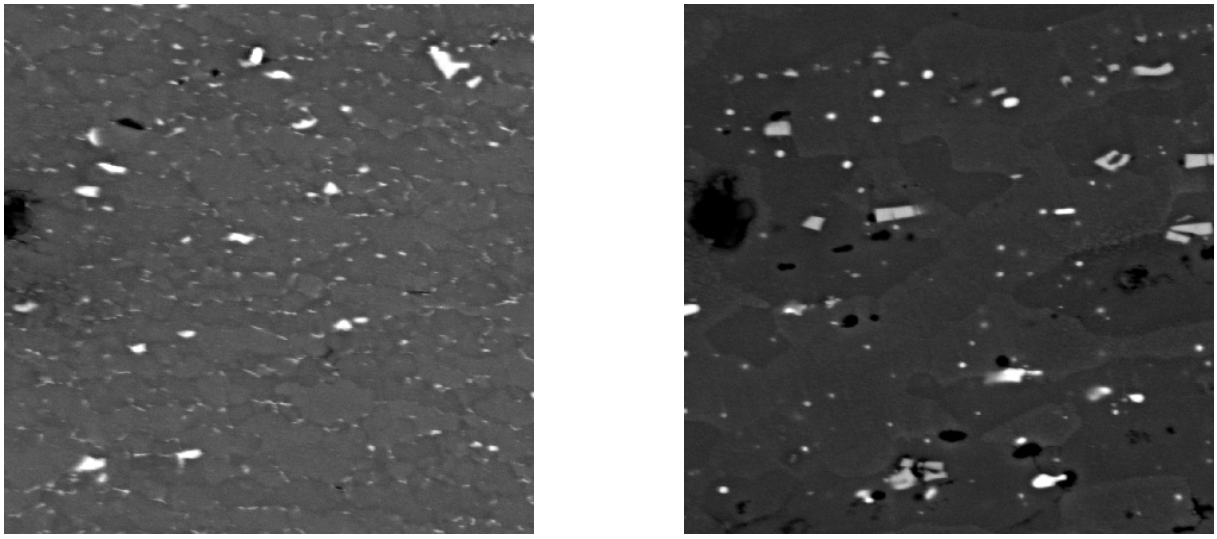

(a) (b)

Fig. 5. SEM micrographs of the friction stir weld nugget zone (a) and the AA2017-T4 aluminum alloy base material (b)

3.2 Micro-hardness

A typical aluminum FSW joint hardness mapping is obtained, see Fig. 6. As expected, the hardness profile takes the form W with the highest values in the nugget zone, and the lowest values in the HAZ. This heterogeneous hardness is a macroscopic signature of the microstructural change due to the extreme deformation undergone by the material and the frictional heat dissipated during welding. Moreover, the heat generated induces a thermal softening and the precipitates dissolution, which lead to the recorded lower values of micro-hardness, similar to the one observed in reference [3]. The microhardness of the zone near the HAZ is lower than that of the nugget zone.

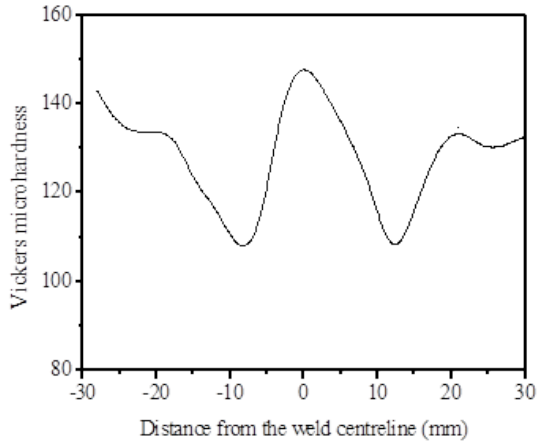

Fig. 6. Microhardness profile across a friction stir weld in AA2017-T4 aluminum alloy

3.3 Tensile test

The stress-strain response of FSW welded and BM specimens, having undergone tensile test with an imposed displacement loading rate of 0.1mm/s, are presented in Fig. 7. Noticeable evolutions of the mechanical properties

are recorded after FSW welding. Hence, the yield stress, the ultimate tensile strength (UTS) and the elongation at failure (UE) as well, summarized in Table 3, are clearly lower for the welded specimen. This may be explained by material and geometrical incompatibilities arising from the welding. In fact, the dynamic recrystallization phenomenon triggered by the heat generated by friction and plastic dissipation increases the size of grain, after getting smaller because of the extreme deformation undergone. The increase in grain size leads to a softer material (lower yield stress), which localizes the deformation in the nugget zone. Besides, the increase in grain size is deemed to allow the appearance of stress concentration. All these provoke the material premature failure. There is also a structural/geometrical factor leading to this premature failure, which is the thickness reduction at the welding joint compared to the base material. Moreover, it has been observed that the tensile specimen failure occurred in the mixing zone between the TMAZ and HAZ. Finally, the recovered UTS and UE of the welded joint are 60% and 18% of the BM values, respectively. Similar observations are reported in references [28, 32].

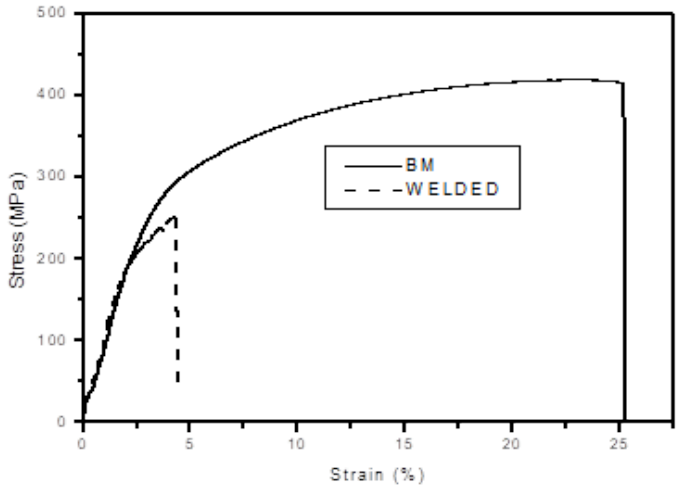

Fig. 7. Stress-strain curves obtained for AA2017-T4 aluminum alloy base metal and friction-stir-welded test coupons

Table 3. Mechanical properties of AA2017-T4 aluminum alloy test coupons without and with a friction stir welded joint

	Tensile strength (MPa)	Yield strength (MPa)	Elongation (%)
Base metal	447	277	19
Welded	268	212	1.95

3.4 Disk Pressure Test - DPT

The welded and BM specimens have been submitted to pressure loading with 25 bar/s applied pressurization rate of inert gas (helium). Fig. 8 displays the failure faces of both specimens (BM and welded) for which the failure occurred by burst with some differences. For BM specimen, the burst is accompanied by fragmentation that gives rise to a “Flower” shape of the failure facies. This is a common feature for ductile materials like the tested aluminum alloy. For the welded specimen, the burst occurs with one sharp failure giving rise to a “Central Cap Outstripping" shape, [33], of the fracture faces in this case. This shape suggests that the weld material is less ductile and undergone partially or totally brittle fracture.

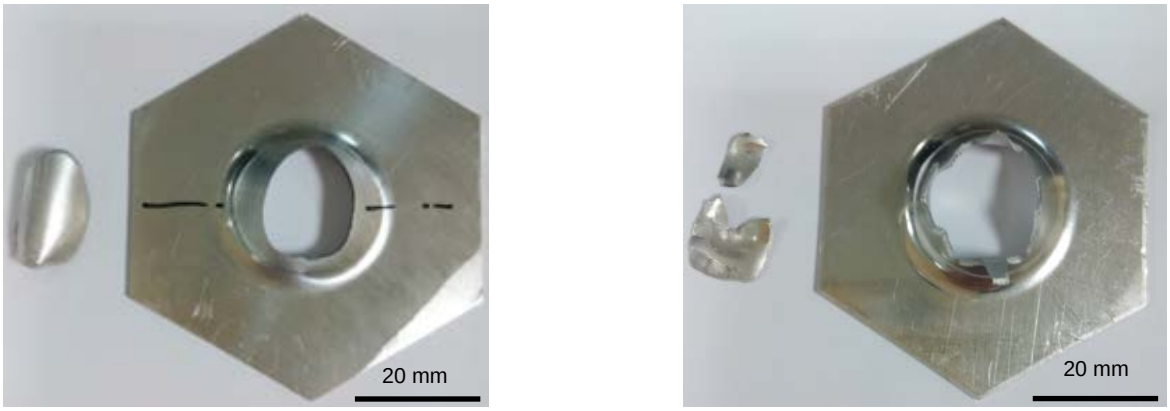

(a) (b)

Figure 8: Disk pressure test (DPT) specimens after testing, a) Welded, b) Base Metal

The fracture faces appear ellipse-like, i.e. more stretched in one direction, in the case of welded specimen, denoting anisotropy deformation. This may be explained by the FSW-induced heterogeneity unlike the BM which is globally homogeneous.

This material heterogeneity after FS welding explains also the early failure of the welded specimen. In fact, low hardness has been measured in HAZ, stating an increase of the grain size in this region following the FS Welding because of the dynamic recrystallization (thermal softening). Hence, grains of large size that can promote stress concentration in HAZ, coexist with finer grains at the TMAZ, giving rise to an interfacial zone, which also induces stress concentration leading to crack initiation and failure [34, 35]. Accordingly, the onset of failure was identified at the interfacial zone between HAZ and TMAZ [34].

Fig. 9 displays the pressure-time responses of the welded and the BM specimens. It shows an earlier failure for the welded specimen than BM. The pressures at failure for both specimens are given in Table 4. The one corresponding to the welded specimen is 66% of that measured for BM specimen.

Table 4. Disk Pressure Test results

	Welded specimen	BM specimen	Efficiency (%)
Failure pressure (bar)	581	700	83

Moreover, it can be observed from Fig. 10, that the thickness reduction of BM specimen is significantly higher than that of the FSWed one. This is consistent with the earlier failure of the welded specimen compared to BM specimen because of the interface effects explained above and a possible increase of the hardening capacity of the welded joint as well.

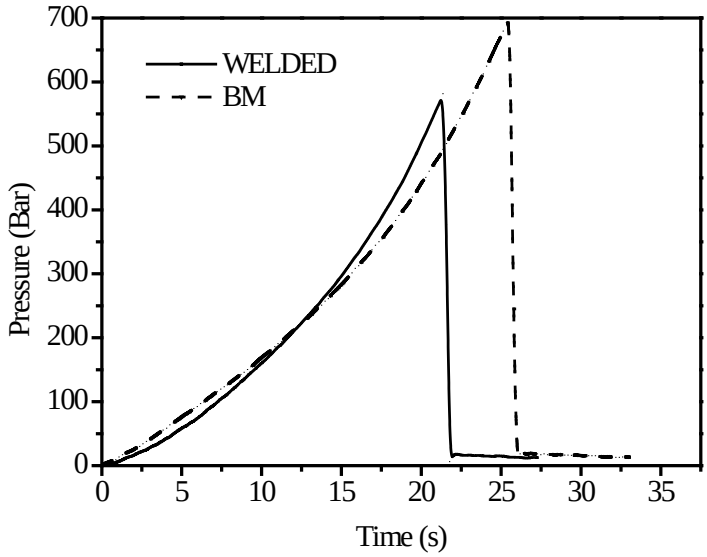

Fig. 9. Time course of the gas pressure withstood by welded AA2017-T4 aluminum alloy compared to the base metal

(a) (b)

Fig. 10. Disc pressure test fracture surface width of (a) welded joint, (b) base material

3.5 Fractography - Disk Pressure Test DPT

Micrographic images of the failure faces were realized on a CAMBRIDGE-360 SEM with an accelerating voltage of 20 keV in a secondary electron mode is presented in Fig. 11. These micro-graphs show dimples, testifying a ductile failure mode for both specimens, even if the sharp shape of the fracture faces for the welded specimen displayed in

Fig. 8 may have suggested a more brittle failure. Moreover, the dimples seem deeper and of higher concentration for BM (Fig. 11b) than for the welding joint (Fig. 11a), which reflects the higher deformability/ductility of the BM compared to welded joint.

The fractured surface average width of the welded specimen is lesser than that of the base metal (BM). The fragments thickness of the welded specimen is measured in the range between 0.98 mm and 1 mm, and that of the base metal (BM), in the range between 0.68 mm and 0.83 mm (Ref. Figs. 10a and 10b), testifying that the base metal specimen deformation is higher than that of the welded specimen. This observation agrees well with micrographic images of the fracture faces given in Figs. 11a and 11b.

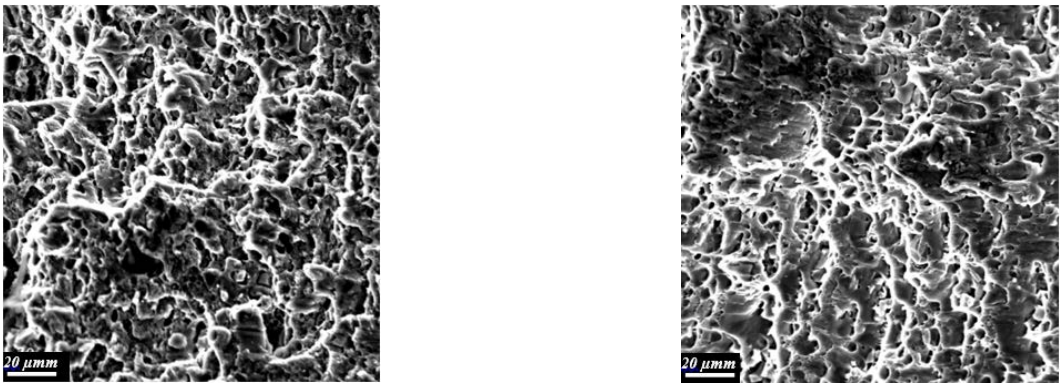

(a) (b)

Fig. 11. SEM micrographs of disc pressure tests fracture surfaces for (a) the welding joint, (b) the BM,

4 CONCLUSION

In this work, 2 mm thick aluminum alloy sheets AA2017-T4 were welded by FSW technique with a conventional milling machine. Surface inspection reveals that the obtained FSW butt welds are free from macroscopic defects. Moreover, a thickness reduction of the welded joints is observed. At the microscopic scale, SEM observations evidenced a grain refining due to recrystallization phenomenon and a re-forming of the precipitates at the nugget zone of the welding joint. The joint section micro-hardness profile, of W-shape, is typical of FSW welds. Tested under a disk pressure bi-axial loading, the AA2017-T4 FSW-welded displayed 83% efficiency compared to the base metal in terms of pressure at failure. The fractured surface of the FSW joints shows a ductile fracture mode for both materials, welded and BM, with relatively deeper and more dimples for the welded joint. After the disc pressure test, the FSW joints strain at failure (thickness reduction) is clearly lower for the welded joint. This difference can be explained by an interface effect that is due to the dissimilarity between the microstructure of the welded joint and the base metal. The difference in efficiency values between the disc pressure test and the tensile test can be due to the effect of the welded joints thickness reduction in the tensile test, which is not in the case for the DPT test.

5 REFERENCES

[1] Thomas, W.M., Nicholas, E.D., Needham, J.C., Murch, M.G., Temple-Smith, P., Dawes, C.J. (1991). Friction stir butt welding. International patent application No. PCT/GB92/02203, 1991.GB Patent No. 9125978.8

[2] Gangwar,K., Ramulu,M. (2018). Friction stir welding of titanium alloys: A review. Materials & Design, vol. 141, 230-255, DOI: 10.1016/j.matdes.2017.12.033

[3] Mishra, R.S., Ma, Z.Y. (2005). Friction stir welding and processing. Materials Science and Engineering, vol. 50, no. 1-2, 1-78, DOI: 10.1016/j.mser.2005.07.001

[4] Kusharjanta, B., Soenoko, R., Purnowidodo, A., Irawan, Y.S. (2022). Analysis of tensile strength, crystallinity, crystallite size, and thermalstability of polypropylene joined by friction stir welding. Journal of Applied Engineering Science, vol. 20, no. 1, 85-90, DOI: 10.5937/jaes0-30899

[5] Eslami, S., Tavares, P.J., Moreira, P.M.G.P. (2017). Friction stir welding tooling for polymers: review and prospects. International Journal of Advanced Manufacturing Technology, vol. 89, no. 5-8, 1677–1690. DOI: 10.1007/s00170-016-9205-0

[6] Raj, A., Pratap Kumar, J., Melwin Rego, A., Sunit Rout, I. (2021). Optimization of friction stir welding parameters during joining of AA3103 and AA7075 aluminium alloys using Taguchi method, Materials Today: Proceedings, vol. 46, no. 17, 7733-7739, DOI: 10.1016/j.matpr.2021.02.246

[7] Hassanifard, S., Ghiasvand, A., Hashemi, S.M., Varvani-Farahani, A. (2022). The effect of friction stir welding tool shape on tensile properties of welded Al 6061-T6 joints. Materials Today: Communications, vol. 31, no. 103457, DOI: 10.1016/j.mtcomm.2022.103457

[8] Sharma, A., Khan, Z. A., Siddiqueeb, A.N. (2022). A short review of the effect of plunge depth on friction stir welding of aluminium pipes. Materials Today: Proceedings, vol. 64, no. 3, 1504-1506, DOI: 10.1016/j.matpr.2022.05.257

[9] Muthumanickam, A., Gandham, P., Dhenuvakonda, S. (2019). Effect of Friction Stir Welding Parameters on Mechanical Properties and Microstructure of AA2195 Al–Li Alloy Welds. Transaction Indian Institute of Metals, vol. 72, no. 6, 1557-1561, DOI: 10.1007/s12666-019-01570-x

[10] Wang, Z.B., He, Z.B., Fan, X.B., Zhou, L., Lin, Y.L., Yuan, S.J. (2017). High temperature deformation behavior of friction stir welded 2024-T4 aluminum alloy sheets. Journal of Materials and Processing Technology, vol. 247, 184-191, DOI: 10.1016/j.jmatprotec.2017.04.015

[11] Tan, M., Wu, C., Su, H. (2023). Ultrasonic effects on microstructures and mechanical properties of friction stir weld joints of dissimilar AA2024/AZ31B alloys. Welding in the World, vol. 67, 373–384, DOI: 10.1007/s40194-022-01429-8

[12] Sánchez Egea A.J., Rodríguez A., Celentano D., Calleja A., López de Lacalle L.N. (2019). Joining metrics enhancement when combining FSW and ball-burnishing in a 2050 aluminium alloy. Surface and Coatings Technology, vol. 367, 327-335, DOI: 10.1016/j.surfcoat.2019.04.010

[13] Ahmed, M.M.Z., Ataya, S., El-Sayed Seleman, M.M., Ammar, H.R., Ahmed, E. (2017). Friction stir welding of similar and dissimilar AA7075 and AA5083. Journal of Materials Processing Technology, vol. 242, 77–91, DOI: 10.1016/j.jmatprotec.2016.11.024

[14] Xu, W., Li, Z., Sun, X. (2017). Effect of Welding Speed on Mechanical Properties and the Strain-Hardening Behavior of Friction Stir Welded 7075 Aluminum Alloy Joints. Journal of Materials Engineering and Performance, vol. 26, no. 4, 1938-1946, DOI: 10.1007/s11665-017-2618-6

[15] Nova Ajay Joseph, R., Jishadh Ahmed, K.A., Mohamed Rizwaan, M., Rajendran, C. (2021). Effect of artificial ageing on microstructural behaviour of friction stir welded AA2014 aluminium alloy joints. Materials Today: Proceedings, vol. 45, no. 2, 891-894, DOI: 10.1016/j.matpr.2020.02.937

[16] Ramamoorthi, R., Yuvaraj, K.P., Gokul, C., Eashwar, S.J., Arunkumar, N., Abith Tamil Dheen, S. (2021). An investigation of the impact of axial force on friction stir-welded AA5086/AA6063 on microstructure and mechanical properties butt joints. Materials Today: Proceedings, vol. 37, no. 2, 3159-3163, DOI: 10.1016/j.matpr.2020.09.050

[17] Mugada, K.K., Adepu, K. (2018). Influence of ridges shoulder with polygonal pins on material flow and friction stir weld characteristics of 6082 aluminum alloy. Journal of Manufacturing Processes, vol. 32, 625-634, DOI: 10.1016/j.jmapro.2018.03.034

[18] Hou, W., Ding, Y., Huang, G. et al. Huda, N., Shah, LHA., Piao, Z., Shen, Y., Shen, Z., Gerlich, A. (2022).The role of pin eccentricity in friction stir welding of Al-Mg-Si alloy sheets: microstructural evolution and mechanical properties. The International Journal of Advanced Manufacturing Technology, vol. 121, 7661–7675, DOI: 10.1007/s00170-022-09793-x

[19] Bozkurt, Y., Boumerzoug, Z. (2018). Tool material effect on the friction stir butt welding of AA2124-T4 Alloy Matrix MMC. Journal of Materials Research and Technology, vol. 7, no. 1, 29-38, DOI: 10.1016/j.jmrt.2017.04.001

[20] Liu, F., Sun, Z., Tuo, Y., Ji, Y., Bai, Y.X. (2020).Effect of shoulder geometry and clamping on microstructure evolution and mechanical properties of ultra-thin friction stir-welded Al6061-T6 plates. The International Journal of Advanced Manufacturing Technology, vol. 106, 1465–1476, DOI: 10.1007/s00170-019-04795-8

[21] Hasan, M.M., Ishak, M., Rejab, M. (2017). Effect of backing material and clamping system on the tensile strength of dissimilar AA7075-AA2024 friction stir welds. The International Journal of Advanced Manufacturing Technology, vol. 91, 3991–4007, DOI: 10.1007/s00170-017-0033-7

[22] Lakshmi, A.A., Kumar, B.S., Kumar, M.N., Vasanth Naik, R. (2022). Hot forming behaviour of tailor welded aluminium (AA6061- AA8011) alloy sheets using friction stir welding. International Journal on Interactive Design and Manufacturing , DOI: 10.1007/s12008-022-00946-6

[23] Kumar, P., Sharma, S. (2021). Influence of FSW Process Parameters on Formability and Mechanical Properties of Tailor Welded Blanks AA6082-T6 and AA5083-O Using RSM with GRA-PCA Approach. Transactions of the Indian Institute of Metals, vol. 74, no. 8, 1943-1968, DOI: 10.1007/s12666-021-02255-0

[24] Ardon, K., Charles, Y., Gaspérini, M., Furtado, J., (2013). A Numerical and Experimental Study of the Disk Pressure Test, ASME 2013 Pressure Vessels and Piping Conference 2013, p. 1-8

[25] Briottet, L., Moro, I., Lemoine, P. (2012). Quantifying the hydrogen embrittlement of pipeline steels for safety considerations. International Journal of Hydrogen Energy, vol. 37, no. 22, 17616-17623, DOI: 10.1016/j.ijhydene.2012.05.143

[26] Sudhagar, S., Sakthivel, M., Mathew, P.J., Daniel, S. A. A. (2017). A multi criteria decision making approach for process improvement in friction stir welding of aluminum alloy. Measurement, vol. 108, 1-8, DOI: 10.1016/j.measurement.2017.05.023

[27] Rajakumar, S., Balasubramanian, V. (2012). Establishing relationships between mechanical properties of aluminium alloys and optimised friction stir welding process parameters. Materials and Design, vol. 40, 17-35, DOI: 10.1016/j.matdes.2012.02.054

[28] Scialpi, A., De Giorgi, M., De Filippis, L.A.C., Nobile, R., Panella, F.W. (2008). Mechanical analysis of ultra-thin friction stir welding joined sheets with dissimilar and similar materials. Materials & Design, vol. 29, no. 5, 928-936, DOI:10.1016/j.matdes.2007.04.006

[29] Su, J.-Q., Nelson, T.W., Mishra, R., Mahoney, M. (2003). Microstructural investigation of friction stir welded 7050- T651 aluminum. Acta Materalia, vol. 51, no. 3, 713-729, DOI: 10.1016/S1359-6454(02)00449-4

[30] Tao, W., Shuwei, D., Matsuda, K., Yong, Z. (2022). Dynamic recrystallization and dynamic precipitation in AA6061 aluminum alloy during friction stir welding. Transactions of the Indian Institute of Metals, vol. 75, no. 5, 1329-1339, DOI: 10.1007/s12666-021-02490-5

[31] Chen, P., Zou, S., Chen, J., Qin, S., Yang, Q., Zhanga, Z., Jia, Z., Zhang, L., Jiang,T., Liu, Q. (2021). Effect of rotation speed on microstructure evolution and mechanical properties of nugget zone in 2195-T8 Al-Li alloy friction stir welding joints. Materials Characterization, vol. 176, no. 111079, DOI: 10.1016/j.matchar.2021.111079

[32] Liu, H.J., Fujii, H., Maeda, M., Nogi, K. (2003). Tensile properties and fracture locations of friction-stir-welded joints of 2017-T351 aluminum alloy. Journal of Materials Processing Technology, vol. 142, no. 3, 692–696, DOI: 10.1016/S0924-0136(03)00806-9

[33] Arnould–Laurent, R., Fidelle J.P. (1981). The disk pressure test – a powerful mechanical investigation method. 5th international conference on rupture 1981, p. 1-16.

[34] Moreira, P.M.G.P., Santos, T., Tavares, S.M.O., Richter-Trummer V., Vilaça,P., de Castro, P.M.S.T. (2009). Mechanical and metallurgical characterization of friction stir welding joints of AA6061-T6 with AA6082-T6. Materials & Design, vol. 30, no. 1, 180-187, DOI: 10.1016/j.matdes.2008.04.042

[35] Khan, N.Z., Siddiquee, A.N., Khan, Z.A., Mukhopadhyay A.K. (2017). Mechanical and microstructural behavior of friction stir welded similar and dissimilar sheets of AA2219 and AA7475 aluminium alloys. Journal of Alloys and Compounds, vol. 695, 2902-2908, DOI: 10.1016/j.jallcom.2016.11.389

Paper submitted: 07.11.2022.

Paper accepted: 05.02.2023.